Electrochemical and spectroelectrochemical characterization of *meso*-tetra-alkyl porphyrins

Carlos Paliteiro[*],[1], Abílio Sobral

Departamento de Química, Universidade de Coimbra, Coimbra 3004-535, Portugal

Abstract

A series of three *meso*-tetra-alkyl porphyrins (H_2TAPs) were synthesised and their electrochemical properties were studied in dichloromethane containing either tetra-butyl ammonium perclorate (TBAP) or tetra-butyl ammonium hexafluorophosphate $TBA(PF_6)$ as supporting electrolyte (SE) by cyclic voltammetry and in situ UV/vis spectroelectrochemistry. Values of $E_{1/2}$ for the recorded four redox processes of these porphyrins and of the *meso*-tetra-phenyl porphyrin (H_2TPP) on glassy carbon and platinum were measured and compared. The redox data collected on the first oxidation and the first reduction processes predict that the value of $\Delta(LUMO - HOMO)$ for the H_2TAPs is lower than for *meso*-tetra-phenyl porphyrin and, therefore, that the first Q band of the electronic spectra of the H_2TAPs is red shifted relatively to the same band in the spectrum of H_2TPP; this shift was indeed found. The second oxidation process of the H_2TAPs is influenced by the supporting electrolyte used and the dication then formed is consumed by an irreversible chemical reaction. The species produced in this reaction is irreversibly reduced at a considerably lower potential. The electrochemical and spectroelectrochemical data collected are consistent with the occurrence of structural distortion in the macrocycle rings of the H_2TAPs.
© 2004 Elsevier Ltd. All rights reserved.

Keywords: *meso*-Tetra-alkyl porphyrins; Molecular electrochemistry; Organic electrochemistry; In situ UV/vis spectroelectrochemistry

1. Introduction

Porphyrins are compounds with considerable importance both from a fundamental and an applied point of view. Their ubiquity in nature is well known and their technological applications spread to a great diversity of areas from medicine to materials science [1–5].

An important part of their interesting reactivity are oxidative processes that, after removal of one or two electrons from the porphyrin core, lead to the formation of the π-cation and dication radicals. These radicals are key intermediates in reactions involving porphyrins and metalloporphyrins, both in nature [6–8] and in the laboratory [9–11]. Therefore, a full knowledge of those redox processes is of great importance in the understanding of the role of the porphyrin macrocycle in the natural or artificial processes of photosynthesis, membrane electron transport or oxygenation catalysis.
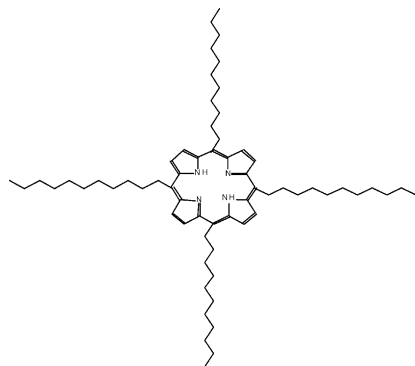
meso-Tetra-alkyl porphyrins are a class of porphyrins with a substitution pattern that lies between the full *meso*-free natural porphyrins and the full *meso*-phenyl-substituted porphyrins of the *meso*-tetra-phenyl porphyrin (H_2TPP) family. Since the *meso* positions are very often involved in the radical processes that are the base of a large number of porphyrin-mediated reactions, and the substitutes at those positions have a determinant role in determining the lifetime and reactivity of the radical intermediates [12–13], the *meso*-tetra-alkyl porphyrins (H_2TAP) can, therefore, be very useful probes for the understanding of the structure/activity relationships of the porphyrin molecules.

With this context in mind, we prepared by the acetic acid/nitrobenzene method [14] the following *meso*-alkyl porphyrins: the *meso*-tetra-(undecyl)- (P1), the *meso*-tetra-
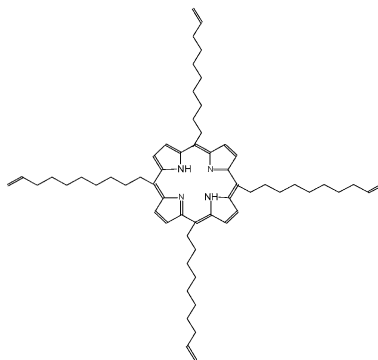
* Corresponding author. Tel.: +351 239852080; fax: +351 239827703.
E-mail address: paliteir@ci.uc.pt (C. Paliteiro).
[1] ISE member.
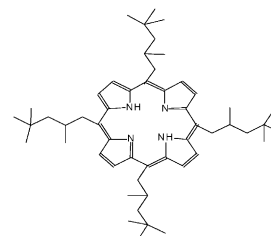
(decyl-9-ene)- (P2) and the *meso*-tetra-(2,4,4-trimethyl-pentyl)-porphyrin (P3). Porphyrins P2 and P3 are new compounds.

P1   **P2**   **P3**

The reports on the redox behaviour of *meso*-tetra-alkyl porphyrins are rather scarce. Fonda et al. studied seven *meso*-substituted porphyrins (two of them were the *meso*-tetra-methyl and the *meso*-tetra-pentyl porphyrins) [15], but their experimental work was mainly directed to the collection of spectroscopic and photophysical data and very few redox potential values were measured.

In this paper, we report and discuss much more extensive data obtained on the electrochemical behaviour of these porphyrins and complement them with in situ UV/vis spectro-electrochemical data. Also, we compare these data with those obtained for the H$_2$TPP in the same experimental conditions.

2. Experimental

2.1. Synthesis of porphyrins

The *meso*-tetra-(undecyl)-porphyrin, P1, and the *meso*-tetra-phenyl porphyrin were prepared and isolated by literature methods [16–17], giving physical data in full agreement to the published values.

The *meso*-tetra-(9-ene-decyl)-porphyrin, P2, and the *meso*-tetra-(2,4,4-trimetil-pentyl)-porphyrin, P3, although made by the same method as that of porphyrin, P1, are new compounds, with the following physical characteristics:

meso-Tetra-(decyl-9-ene)-porphyrin (P2): yield of 6%. Mass spectrum: FAB+, M+ at *m/z* 863. Elemental analysis: expected for C$_{60}$H$_{86}$N$_4$: (C: 83.47%; H: 10.04%; N: 6.49%). Found: (C: 83.54%; H: 9.29%; N: 6.30%). Melting point: 79–80 °C. UV/vis spectrum: (CH$_2$Cl$_2$) (nm; % of Soret band) = (417; 100%), (520; 5.3%), (555; 4.3%), (598; 2.8%), (658; 3.6%). UV/vis spectrum for the dication: (CH$_2$Cl$_2$; TFA 5%) (nm; % of Soret band) = (424; 100%), (589; 7.5%), (635; 11%). ^{1}H RMN (CDCl$_3$/TMS; ∂ in ppm): (9.1; 8H; s; *H*β), (5.7; 4H; m; –C*H*=CH$_2$), (4.9; 8H; m; –CH=C*H*$_2$), (4.8; 8H; t; ring –C*H*$_2$–CH$_2$–), (1.1–2.1; 56H: m; –CH$_2$–(C*H*$_2$)$_7$–CH–), (−2.7; 2H; s, NH).

meso-Tetra-(2,4,4-trimethyl-pentyl)-porphyrin (P3): yield of 8%. Mass spectrum: FAB+, (M+H)+ at *m/z* 760. Elemental analysis: expected for C$_{52}$H$_{78}$N$_4$: (C: 82.27%; H: 10.35%; N: 7.38%). Found: (C: 81.97%; H: 9.80%; N: 6.97%). Melting point: 215–220 °C. UV/vis spectrum: (CH$_2$Cl$_2$) (nm; % of Soret band) = (419; 100%), (521; 5%), (556; 4%), (600; 2.4%), (660; 3%). UV/vis spectrum for the dication: (CH$_2$Cl$_2$; TFA 5%) (nm; % of Soret band) = (427; 100%), (590; 8%), (634; 12%). ^{1}H RMN (CDCl$_3$/TMS; ∂ in ppm): (9.2; 8H; s; *H*β) (4.6; 8H; d; ring –C*H*$_2$–CH–) (1.7–1.3; 12H; m; –C*H*$_2$–(CH$_3$)–C*H*–) (1.1; 12H; d; –C*H*$_3$) (0.8; 36H; s; –(C*H*$_3$)$_3$) (−2.8; 2H; s, NH).

2.2. Solvents and materials

Dichloromethane was chosen as the porphyrins solvent. It was distilled from CaCl$_2$ and stored over 3 Å molecular sieves. The amount of the solvent necessary for the preparation of the solutions were passed through a column of dry alumina (Fluka, chromatographic grade) with a thin layer of K$_2$CO$_3$ (Merck, purissimum) under an argon (99.99%, Air Liquide) atmosphere.

In the experiments, electrochemical grade tetra-butyl ammonium salts (Fluka), either perclorate (TBAP) or hexafluorophosphate (TBA(PF$_6$)), were used as supporting electrolytes (SE) without further purification. Ferrocene (Merck) was added to the porphyrin solution in the end of the experiments to use its potential of oxidation as an internal potential standard. Solutions of Ag$^+$ in acetonitrile were prepared from Analar AgNO$_3$ (BDH) and chromatographic grade acetonitrile (Merck). All the solid reagents were dried and kept in an excicator under reduced pressured before use.

2.3. Electrochemical experiments

Cyclic voltammetric measurements were made by using a PAR 273A potentiostat (controlled by PAR M270 software) and a Metrohm electrochemical cell with a thermostatic jacket; this cell was placed in a Faraday cage. Experiments were performed at 20 °C. Either a Pt ring or a glassy carbon (GC) disc was used as the working electrode (WE) and a Pt mesh was the auxiliary electrode (AE). An Ag wire dipped

in a 0.01 M Ag$^+$ acetonitrile solution also 0.1 M in the SE, served as the reference electrode (RE). Both the RE and the AE were separated from the porphyrin solution by a glass bridge with a Vycor tip containing a 0.1 M solution of the SE in dichloromethane. Although the potential was measured relatively to an Ag|0.01 M Ag$^+$, 0.1 M SE, CH$_3$CN||reference system, they are referred to the potential of the ferrocinium ion/ferrocene (Fc$^+$/Fc) couple used as an internal standard. The measured value of the $E_{1/2}$ of this couple relatively to the Ag/Ag$^+$ reference system was 228 mV ($E_{1/2}$ represents half the sum of the potentials of the oxidation and the reduction peaks correspondent to a given redox process).

2.4. Spectroelectrochemical experiments

The spectroelectrochemical cell was a commercial spectrophotometric cell (Hewlett-Packard) with a 1 mm optical pathlength that was modified in its top in order to accommodate the WE, the RE and the AE electrodes, in an arrangement very similar to that used in Anson's lab [18]. The WE was a Pt mesh placed in the optical path and was, therefore, crossed by the light beam; the RE was an Ag wire dipped in a 0.01 M Ag$^+$ acetonitrile solution which was also 0.1 M in the supporting electrolyte (always TBA(PF$_6$)) separated from the porphyrin solution by a glass bridge with a Vycor tip containing a 0.1 M solution of the supporting electrolyte in dichloromethane; the AE was a platinum spiral placed in this same solution of the supporting electrolyte contained in a glass bridge with a Vycor tip. The cell was installed in the cell holder of a Hitachi model 124 UV/vis spectrophotometer and the absorbance versus wavelength data were collected and stored in a computer with the help of a PCI-GPIB board and LabView 5.0 software both from National Instruments. In these experiments, the potential applied to the WE was controlled by a PAR 263 potentiostat.

3. Results and discussion

3.1. Electrochemical experiments

3.1.1. Redox processes: general data

Fig. 1 shows the cyclic voltammograms (CV) of the alkyl porphyrin P1 in CH$_2$Cl$_2$ (the CVs for P2 and P3 are similar to that recorded for P1), and compares it with the CV recorded for H$_2$TPP in the same experimental conditions which is in agreement with that reported in the literature [19]. All the CVs in Fig. 1 are net CVs obtained after subtraction of the CVs recorded in the absence of the porphyrin.

The H$_2$TAPs show a very similar electrochemical behaviour, which differs from that recorded for the H$_2$TPP. Four electrochemical reversible processes involving one electron per porphyrin molecule are observed in all cases, corresponding to the oxidation of the porphyrin followed by the oxidation of the π-cation formed and to the reduction of the porphyrin followed by the reduction of the π-anion formed. Table 1
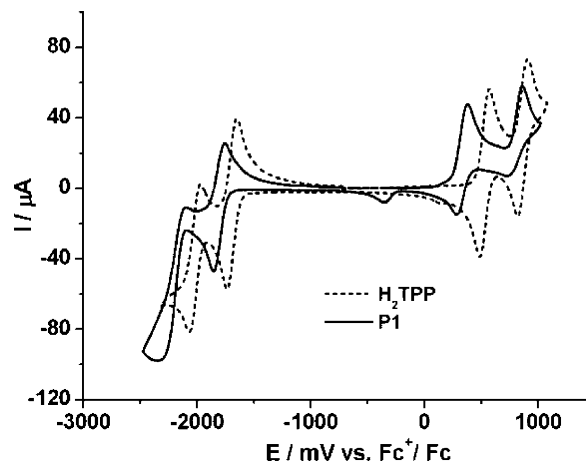

Fig. 1. CVs obtained on Pt in an argon-saturated CH$_2$Cl$_2$ solution about 1 mM in the porphyrin and 0.1 M in TBA(PF$_6$). Scan rate: 50 mV s^{-1}.

summarises the electrochemical information obtained in this work.

The data reported in Table 1 support the following conclusions:

(a) The values of the $\Delta E_{1/2}$**1-2** and **3-1** measured for the H$_2$TAPs studied in this work fall, respectively, in the range 0.42 ± 0.05 V and 2.25 ± 0.15 V, whereas the value of $\Delta E_{1/2}$**4-3** measured in a TBAP solution with a Pt WE is very close to the upper limit of the 0.29 ± 0.05 V range. These potential ranges are characteristic of processes occurring in the porphyrin ring [20], and were also verified in the experiments on H$_2$TPP.

(b) The $E_{1/2}$ of the oxidation process of the H$_2$TAPs are about 200 mV more cathodic than that of H$_2$TPP. They are, therefore, more easily oxidised than the H$_2$TPP, which was expected considering the donor versus the acceptor character of, respectively, the alkyl and the phenyl groups.

(c) As also expected, therefore, the $E_{1/2}$ of the reduction process of the H$_2$TAPs are about 100 mV more cathodic than that of H$_2$TPP; they are then less reducible than H$_2$TPP.

(d) Relatively to the $E_{1/2}$ of the same processes in the H$_2$TPP, the cathodic shift of the $E_{1/2}$ for the first reduction process, **1**, of the H$_2$TAPs studied is, therefore, smaller than the observed cathodic shift of the $E_{1/2}$ for their first oxidation process, **3**. As the $\Delta E_{1/2}$**3-1** is a good estimate of the energy separation between the HOMO and the LUMO of the reacting molecule [21], we expect that such separation in the H$_2$TAPs is smaller than in H$_2$TPP and that, therefore, the first Q band of the visible spectra of those porphyrins is shifted to the red relatively to the same band of the H$_2$TPP visible spectrum. As shown in Section 3.2, such shift was indeed observed in this work and also in work done by other workers on *meso*-H$_2$TAPs [15].

(e) The considerable cathodic shift ($\approx$200 mV) of the peak potential of the second oxidation process of the H$_2$TAPs relatively to the peak potential of the same process for H$_2$TPP points to the destabilization of their π-cations

Table 1
$E_{1/2}$ measured at 20 mV s^{-1} for the redox processes of porphyrins P1, P2, P3 and H$_2$TPP in a CH$_2$Cl$_2$/ES solution

Porphyrins	ES	$E_{1/2}$/V vs. Fc$^+$/Fc				$\Delta E_{1/2}$/V		
		1	2	3	4	1–2	4–3	3–1
Glassy carbon								
P1	TBAP	−1.79	−2.18	0.32	0.74	0.39	0.42	2.11
	TBA(PF$_6$)	−1.80	−2.19	0.33	0.80	0.39	0.47	2.12
P2	TBA(PF$_6$)	−1.80	−2.19	0.33	0.80	0.39	0.47	2.13
P3	TBA(PF$_6$)	−1.81	−2.20	0.34	0.81	0.39	0.47	2.15
H$_2$TPP	TBA(PF$_6$)	−1.69	−2.01	0.53	0.87	0.32	0.34	2.22
Platinum								
P1	TBAP	−1.79	−2.18	0.32	0.68	0.39	0.36	2.11
	TBA(PF$_6$)	−1.80	−2.19	0.33	0.79	0.39	0.46	2.13
P3	TBAP	−1.81	−2.19	0.34	0.69	0.37	0.35	2.15
	TBA(PF$_6$)	−1.82	−2.20	0.33	0.80	0.38	0.47	2.15
H$_2$TPP	TBA(PF$_6$)	−1.69	2.02	0.53	0.86	0.33	0.33	2.22

(1–4) Indicate the redox processes: 1, porphyrin/π-anion; 2, π-anion/π-dianion; 3, porphyrin/π-cation; 4, π-cation/π-dication.

(i.e., points to a higher energy of their HOMO). A decrease of the Δ(LUMO − HOMO) of a porphyrin together with a destabilization of its π-cation, was correlated with structural data on the deformation of the porphyrin ring from a planar to a saddle configuration [22]. It is then probable that the alkyl porphyrins P1, P2 and P3 studied in this work are structurally deformed. Fonda et al. [15] arrived at the same conclusion in their study of *meso*-substituted porphyrins (tetra-methyl- and tetra-pentyl-).

(f) The $E_{1/2}$ of the different redox processes of the H$_2$TAPs are practically the same for the same ES. Changing from solution CH$_2$Cl$_2$/TBA(PF$_6$) to solution CH$_2$Cl$_2$/TBAP does not alter processes 1, 2 and 3 but significantly affects the oxidation of their π-monocations, both on GC and on Pt (cf. Fig. 2 a and b). As a consequence, the value of the $\Delta E_{1/2}$**4-3** decreases about 120 mV when the ES is changed from TBA(PF$_6$) to TBAP. Such a dependence from the ES anion was also observed before by other workers with ZnTPP in CH$_2$Cl$_2$ solutions of the same ES [23,24] and by us with H$_2$TPP in CH$_2$Cl$_2$/TBA(PF$_6$) and CH$_2$Cl$_2$/TBA(tetra-fluoroborate) solutions [25]. Chang et al. justify this dependence with "differences in adsorption characteristics of the complexes between the two SE systems" [Reference 24, p. 819]. This explanation is difficult to understand. In fact, if the porphyrin adsorbs and this adsorption is SE dependent, we would eventually observe instead a separation between the values of the $E_{1/2}$ of the *first* oxidation of the porphyrin measured in the solutions of each SE. However, these values are practically the same.

We propose instead the following explanation: (i) the π-cation formed in the first oxidation process interacts with the SE anion and forms a new species, the ion-pairs {P$^+$(ClO$_4$$^-$)} or {P$^+$(PF$_6$$^-$)}, where P represents the neutral porphyrin molecule, and (ii) the energy of the HOMO of the {P$^+$(ClO$_4$$^-$)} species is higher than that of the HOMO of

the {P$^+$(PF$_6$$^-$)} species, i.e., the stabilization of P$^+$ through ion-pairing increases when the SE anion is changed from ClO$_4$$^-$ to PF$_6$$^-$.

The new species adsorbs on the WE surface giving rise to a stabilized surface species; as a consequence, the first oxi-
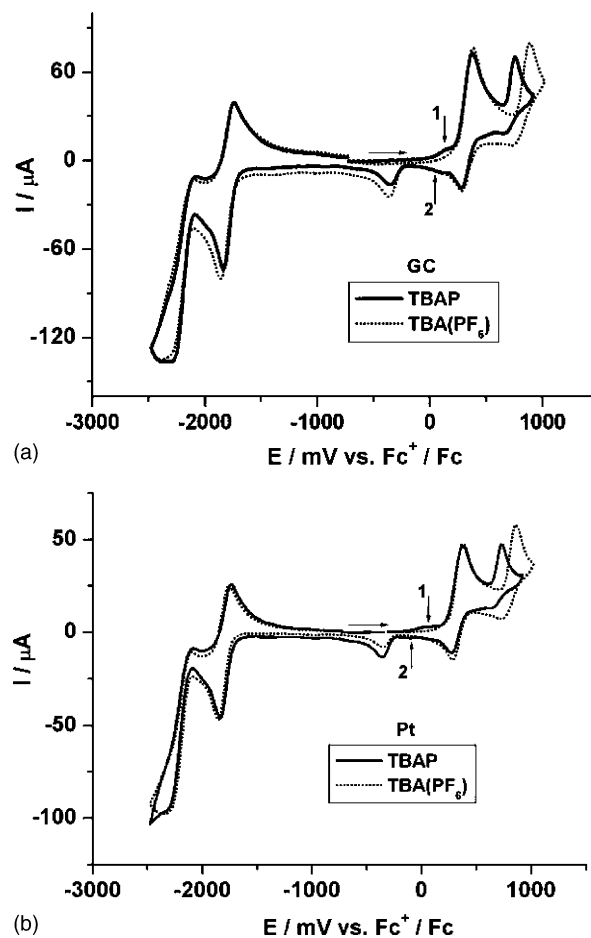

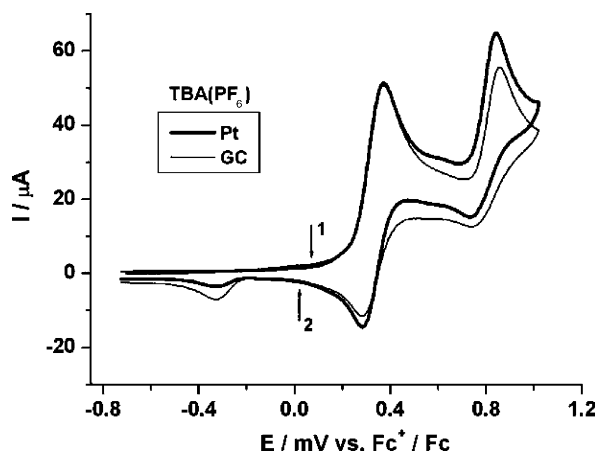Fig. 2. CVs obtained on (a) GC and (b) Pt in an argon-saturated CH$_2$Cl$_2$ solution 1 mM in P1 and 0.1 M in TBAP or in TBA(PF$_6$). Scan rate: 50 mV s^{-1}.

Fig. 3. CVs recorded on GC or Pt in an argon-saturated CH_2Cl_2 solution 1 mM in P1 and 0.1 M in $TBA(PF_6)$. Scan rate: 20 mV s^{-1}.

dation peak Ox1 is preceded by the prewave 1 and followed by the postwave 2 shown in Fig. 2a and b; the adsorption of $\{P^+(ClO_4^-)\}$ is stronger than that of $\{P^+(PF_6^-)\}$ both on GC and on Pt (cf. Fig. 2a and b) and the two adsorption processes are stronger on Pt than on GC (cf. Fig. 3). If the HOMO of $\{P^+(ClO_4^-)\}$ is higher than that of the HOMO of $\{P^+(PF_6^-)\}$, the oxidation of the π-cation will occur, as observed, at a less anodic potential with TBAP than with $TBA(PF_6)$. A lower oxidation potential was also observed on Pt than on GC, cf. Fig. 3, which points to a different interaction between each of these WE surfaces and the $\{P^+(ES^-)\}$ species. Additionally, as the first Q band of the visible spectrum of the π-cation of the H_2TAPs shows a shift to the blue relatively to the same band of the H_2TPP (cf. Section 3.2), we can predict that the difference $\Delta(LUMO - HOMO)$ of the π-cation of the H_2TAPs is greater than the $\Delta(LUMO - HOMO)$ of the π-cation of H_2TPP. This would be consistent with the higher ability of the aromatic system of the H_2TPP to accommodate the positive charge of the π-cation, since its extension is greater than that of the H_2TAPs.

3.1.2. The oxidation processes

Fig. 4 a and b shows more clearly the prewave 1 and the postwave 2 associated to the adsorption of the π-cation. When the reverse potential of the anodic scan is fixed in the potential range where this cation is oxidised to the π-dication (or, more probably, the $\{P^{2+}2(PF_6^-)\}$ ion-pair), a new peak, 3, forms at about -350 mV. The intensity of this peak increases up to a maximum as the reverse potential becomes more anodic and, simultaneously, the intensity of the reduction peak of the π-cation decreases. Additionally, the peak current intensity of the dication reduction, $[(I_p)_4]_{red}$, is lower than that of the corresponding monocation oxidation peak, $[(I_p)_4]_{ox}$, and this current intensity corresponds to less than one electron per monocation.

Together, these observations suggest the occurrence of a chemical reaction that consumes the dication and produces a species that is then reduced at about -350 mV. The ra-

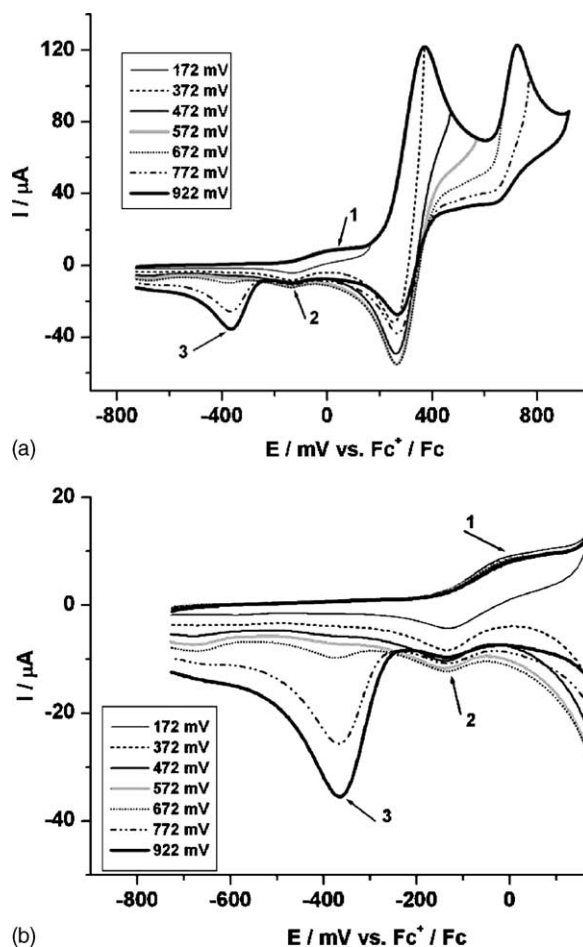Fig. 4. (a) CVs recorded on Pt in an argon-saturated CH_2Cl_2 solution 1 mM in P1 and 0.1 M in $TBA(PF_6)$. Scan rate: 50 mV s^{-1}. $E_{initial}$: -730 mV; E_{final}: several values between 172 and 922 mV. (b) Enlargement of (a) between -730 and 175 mV.

tio $[(I_p)_4]_{red}/[(I_p)_4]_{ox}$ is less than 1 and increases to 1 when the scan rate, v, increases from 20 to 200 mV s^{-1}; additionally, the ratio $[(I_p)_4]_{ox}/v^{0.5}$ is independent of v in the 20–100 mV s^{-1} range. These facts are consistent with the occurrence of an irreversible chemical reaction following the formation of the dication.

To the peak 3 related to the reduction of the species produced in this chemical process, does not correspond any oxidation peak (cf. Fig. 5), i.e., the process is totally irreversible.

It appears to us that this process may be either a dimerization or the degradation of the dication radical macrocycle. Since the use of free base porphyrins rules out the formation of a μ–oxo dimer, so frequent in the metalloporphyrin chemistry, peak 3 might be related to a dimer due the formation of a new π–π′ bond or of a new *meso*-carbon–carbon bond between the dication radical and the free base porphyrin present, as noted by Fuhrhop et al. [27]. However, we cannot exclude the hypothesis of a quick degradation of the dication macrocyle to a reducible biliar pigment analog. Some porphyrin radicals from hindered porphyrins are stable for hours but those from unsubstituted porphyrins, like porphine, are
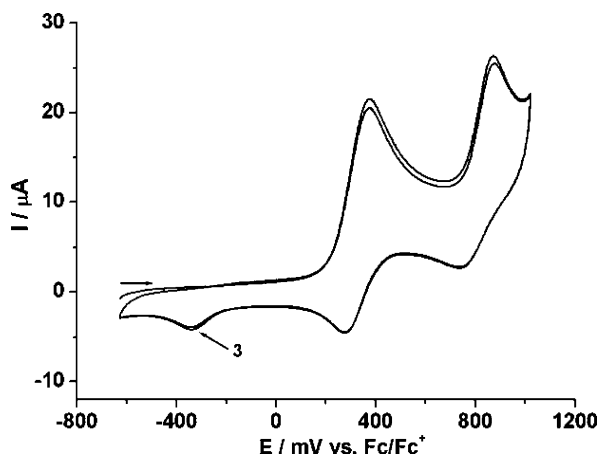
Fig. 5. CVs recorded on GC in an argon-saturated CH_2Cl_2 solution 1 mM in P1 and 0.1 M in $TBA(PF_6)$. Scan rate: $50\,mV\,s^{-1}$.

strong electrophyles that react with any available electron source (namely the porphyrin free base) to produce black precipitates [28]. That may be the case of the *meso*-alkyl porphyrins, whose oxidised species should be less stable than those derived from the *meso*-phenyl porphyrins like TPP.

3.2. In situ spectroelectrochemical experiments

The UV/vis spectra of the porphyrins P1, P2 and P3 show, like that of the H_2TPP, one Soret (S) band and four Q bands (Q1–Q4) (cf. Fig. 6).

The S bands of the H_2TPP and of P1 and P2, (cf. Fig. 6a), have a maximum at 416 nm and a shoulder at 398 nm; the S band of P3 is thinner and both the maximum and the shoulder show a shift, small (about 2 nm) but reproducible, to the red.

The bands Q1–Q4 of the H_2TPP, (cf. Fig. 6b), show maxima, respectively, at 645, 588, 548 and 513 nm. Together with the respective S band, these Q bands give a H_2TPP spectrum with a shape entirely similar to that reported by Fonda et al. [15], which was recorded in benzene and shows values of the λ_{max} of the S and Q bands also practically the same as those found in this work.

Relatively to the Q bands of H_2TPP, those of the H_2TAPs (practically independent of the porphyrin) shift to the red. The value of this shift for the Q1 and Q2 bands (13 and 16 nm, respectively) is greater than that for the Q3 and Q4 bands (about 5 nm). The red shift of the Q1 band of P1–P3 (i) is consistent with the different colour of the solutions of these porphyrins, pink for P1–P3, purple for H_2TPP; (ii) confirms the conclusion reached in Section 3.1 that the difference between the LUMO and the HOMO would be greater for H_2TPP than for the alkyl porphyrins.

When the H_2TPP is oxidised to produce the corresponding monocation, the intensity of the original S band at 416 nm considerably decreases and this band becomes a shoulder of a new band with a maximum at 436 nm (cf. Fig. 7a). On the other hand, the S bands of the monocations of the porphyrins P1–P3 show a maximum at 416 nm, like the corresponding
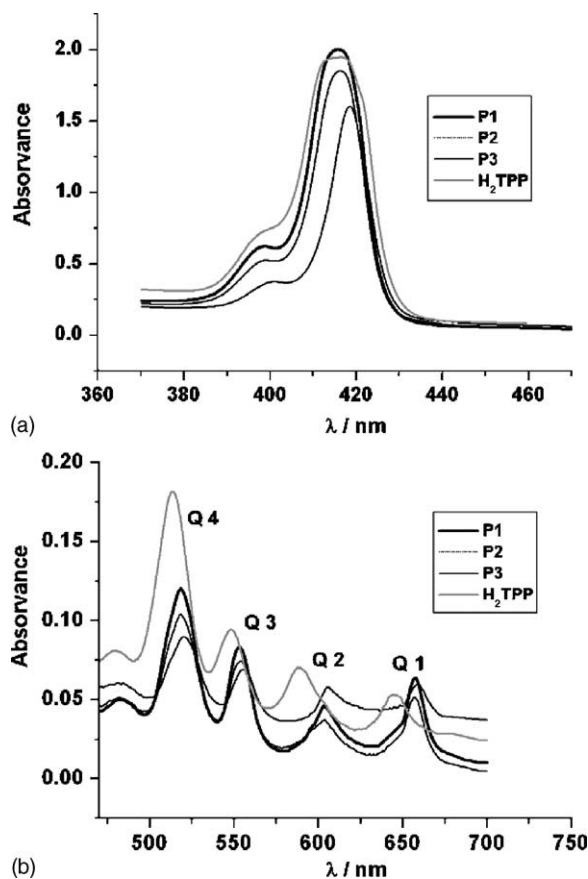

Fig. 6. UV/vis spectra of the alkyl porphyrins P1–P3 and of H_2TPP dissolved (10 μM) in an argon-saturated 0.1 M solution of $TBA(PF_6)$ in CH_2Cl_2. (a) Soret bands; (b) Q bands.

neutral porphyrin, but the intensity of this maximum considerably decreases (specially for P3) and a new shoulder develops at 430 nm (cf. Fig. 7a).

Relatively to those of the original porphyrin, the intensity of the Q2–Q4 bands of the monocations spectra considerably decrease (specially those of the monocation of P3) but the values of λ_{max} are the same (cf. Fig. 7b with Fig. 6a). The corresponding Q1 bands, (i) increase in intensity for all porphyrins (especially for H_2TPP); (ii) show maxima shifted between 20 and 25 nm to the blue in the H_2TAPs and about 9 nm to the red in the H_2TPP.

On the other hand, compared to the same band of H_2TPP, the Q1 bands of the monocations of the H_2TAPs are shifted to the blue by about 25 nm. The electrochemical data collected, cf. Section 3.1, appear to show that the monocation of the porphyrins P1–P3 is destabilized relatively to that of H_2TPP, i.e., the energy level of its HOMO is raised due to a deformation of its porphyrin ring. As the energy of the Q1 band of the monocation of the H_2TAPs is higher than the energy of the same band for H_2TPP, it is predictable that the LUMO of the porphyrins P1–P3 is also greater than the LUMO of the H_2TPP, so that the difference $\Delta(LUMO - HOMO)$ in the monocation of the H_2TAPs is greater than that in the monocation of the H_2TPP.
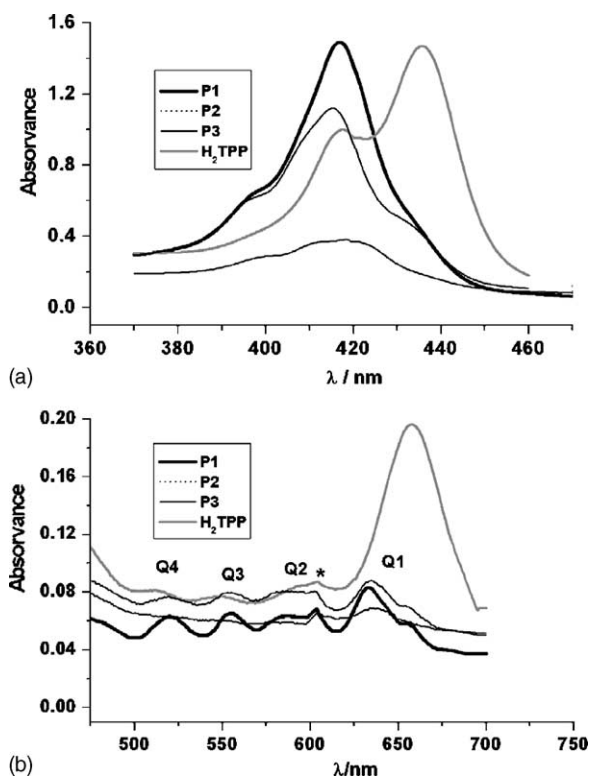
Fig. 7. UV/vis spectra of the π-cation of the alkyl porphyrins P1–P3 and of H_2TPP dissolved (10 μM) in an argon-saturated 0.1 M solution of TBA(PF$_6$) in CH_2Cl_2. (a) Soret bands; (b) Q bands. Applied potentials: H_2TPP: 750 mV; alkyl porphyrins: 520 mV. *Experimental artefact from the spectrophotometer.

4. Conclusions

As expected from the inductive electron donor behaviour of the alkyl groups in contrast with the acceptor nature of the phenyl groups, the H_2TAPs studied in this work are more easily oxidised and more difficult to reduce than the H_2TPP. The electrochemical data collected on the first oxidation and the first reduction processes predict a lower value of $\Delta(LUMO - HOMO)$ for the H_2TAPs than for H_2TPP and, therefore, a shift to the red of the first Q band of the electronic spectra of the H_2TAPs relatively to the same band in the spectrum of H_2TPP; this shift was indeed found. The second oxidation process of the H_2TAPs is SE dependent, which points to the formation of a $P^+(ES)^-$ species, with $\{P^+(ClO_4^-)\}$ more easily oxidised (higher HOMO energy) than $\{P^+(PF_6^-)\}$. The H_2TAPs dication is consumed by an irreversible chemical reaction that produces a species (either a dimer or a product of the dication degradation) then irreversibly reduced at a considerably lower potential. The electrochemical and spectroelectrochemical data collected are consistent with the occurrence of structural distortion of the macrocycle rings of the H_2TAPs.

References

[1] L.F.T. Eyck, in: D. Dolphin (Ed.), The Porphyrins, vol. 7, Academic Press, New York, 1978 (Chapter 10).
[2] O.T.G. Jones, in: D. Dolphin (Ed.), The Porphyrins, vol. 6, Academic Press, New York, 1978 (Chapter 3).
[3] J.H. Chou, H.S. Nalwa, M.E. Kosal, N.A. Rakowa, K. Suslick, in: K. Kadish, K.M. Smith, R. Guilard (Eds.), The Porphyrin Handbook, vol. 6, Academic Press, New York, 2000 (Chapter 41).
[4] R.K. Pandey, G. Zheng, in: K. Kadish, K.M. Smith, R. Guilard (Eds.), The Porphyrin Handbook, vol. 6, Academic Press, New York, 2000 (Chapter 43).
[5] T. Malinski, in: K. Kadish, K.M. Smith, R. Guilard (Eds.), The Porphyrin Handbook, vol. 6, Academic Press, New York, 2000 (Chapter 44).
[6] D. Dolphin, R.H. Felton, Acc. Chem. Res. 7 (1974) 26.
[7] J.H. Fuhrhop, D. Mauzerall, J. Am. Chem. Soc. 91 (1969) 4174.
[8] J. Fajer, D.C. Borg, A. Forman, D. Dolphin, R.H. Felton, J. Am. Chem. Soc. 92 (1970) 3451.
[9] A. Wolberg, J. Manassen, J. Am. Chem. Soc. 92 (1970) 2982.
[10] A. Salehi, W.A. Oertling, G.T. Badcock, C.K. Chang, J. Am. Chem. Soc. 108 (1986) 5630.
[11] P. Gans, G. Buisson, E. Duee, J.-C. Marchon, B.S. Erler, W.F. Scholz, C.A. Reed, J. Am. Chem. Soc. 108 (1986) 1223.
[12] A.J.F.N. Sobral, A.M.d'A. Rocha Gonsalves, J. Porphyrins Phtalocyanines 5 (2001) 428.
[13] A.J.F.N. Sobral, A.M.d'A. Rocha Gonsalves, J. Porphyrins Phtalocyanines 5 (2001) 861.
[14] A.M.d'A. Rocha Gonsalves, M.M. Pereira, J.M.B.T. Varejão, Heterocycl. Chem. 28 (1991) 635.
[15] H.N. Fonda, J.V. Gilbert, R.A. Cornier, J.R. Sprague, K. Kamioka, J.S. Connolly, J. Phys. Chem. 97 (1993) 7024.
[16] A.D. Adler, F.R. Longo, J.D. Finarelli, J. Golmacher, J. Assour, L. Korsakoff, J. Org. Chem. 32 (1967) 476.
[17] H.D. Burrows, A.M.R. Gonsalves, M.L.P. Leitão, M.G. Miguel, Supramol. Sci. 4 (1997) 241.
[18] M. Yuasa, B. Steiger, F.C. Anson, J. Porphyrins Phtalocyanines 1 (1997) 181.
[19] K. Kadish, M.M. Morrison, J. Am. Chem. Soc. 98 (1986) 435.
[20] K. Kadish, Prog. Inorg. Chem. 34 (1986) 435.
[21] E. Gudowska-Nowak, M.D. Newton, J.J. Fajer, J. Phys. Chem. 94 (1990) 5795.
[22] K.M. Barkigia, M.W. Renner, L.R. Furenlid, C.J. Medforth, K.M. Smith, J. Fajer, J. Am. Chem. Soc. 115 (1993) 3627.
[23] E.C. Johnson, T. Niem, D. Dolphin, Can. J. Chem. 56 (1978) 1381.
[24] D. Chang, Y. Malinski, A. Ulman, K.M. Kadish, Inorg. Chem. 23 (1984) 819.
[25] C. Paliteiro, A. Sobral, unpublished results.
[27] J.H. Fuhrhop, P. Wasser, D. Riesner, D. Mauzerall, J. Am. Chem. Soc. 94 (1972) 7996.
[28] J.-H. Fuhrhop, in: K.M. Smith (Ed.), Porphyrins Metalloporphyrins, Elsevier, 1976 (Chapter 14).